

PECULIAR VELOCITY AND DEABERRATION OF THE SKY

D. MENZIES AND G. J. MATHEWS

Department of Physics, University of Notre Dame, South Bend,
 IN 46556; dmenzies@nd.edu, gmathews@nd.edu

Received 2004 September 7; accepted 2005 January 18

ABSTRACT

Recent studies have found the earth’s peculiar velocity to be significant in microwave-background–based tests for compact cosmic topology, and modifications to these tests have been proposed. Tests of non-Gaussianity, weak-lensing analysis, and new tests using improved cosmic microwave background (CMB) data will also be sensitive to peculiar velocity. We propose here to simplify matters by showing how to construct a deaberrated CMB map to which any test requiring a Hubble flow view point can be applied without further complication. In a similar manner, deaberration can also be applied to object surveys used, for example, in topological searches and matter distribution analysis. In particular, we have produced a revised list of objects with $z > 1.0$ using the NASA/IPAC Extragalactic Database.

Subject headings: cosmic microwave background — large-scale structure of universe —
 quasars: general — relativity

1. INTRODUCTION

The peculiar velocity of the Earth relative to the Hubble flow causes a direction aberration and a Doppler shift of light that would be received by a coincident observer moving with the Hubble flow. Given the current precise estimate of the earth’s peculiar velocity from cosmic microwave background (CMB) dipole measurement, $(l, b) \approx (264.3, 48.0)$, $\beta \approx 0.00123$ (Lineweaver 1997), the maximum angular error is $\approx 0.07^\circ$ (Levin 2004). This is enough to cause concern for example in topological searches (Levin 2004; Calvao 2004), weak-lensing, and non-Gaussianity analysis (Challinor & van Leeuwen 2002) based on future CMB measurements. The impact of aberration on the CMB power spectrum is much less significant (Challinor & van Leeuwen 2002). Moreover, in analyses using object surveys, such as topological searches and matter distribution analysis, the aberration is already important, since object positions are available to high accuracy. In the following, the term “aberration” includes the Doppler effect due to the peculiar motion of the Earth relative to the Hubble flow, unless otherwise indicated. We summarize how to make these corrections, and present a new deaberrated table of objects with $z > 1$.

2. CMB DEABERRATION

To deal with aberration, for example in the case of the “circle test” for evidence of cosmic topology (Cornish et al. 1998), modifications have been proposed to these tests (Levin 2004; Calvao 2004). An alternative approach, however, is to construct the view for an observer moving with the Hubble flow observer once, before applying any tests. Any further analysis can proceed as before unaltered, without the trouble of deriving and verifying modified tests that may require considerably increased computer time. This deaberration can be achieved by calculating the view of an observer moving with velocity $-\beta$ relative to the earth, where β is the peculiar velocity of the earth relative to the Hubble flow. In other words, we aberrate our Earth view with a velocity $-\beta$. This scheme is illustrated in Figure 1.

A light ray, viewed along the line of sight \hat{n} with a direction 3-vector $-\hat{n}$, is aberrated by velocity β as (Calvao 2004)

$$\hat{n}' = \frac{\hat{n} + [(\gamma - 1)\hat{\beta} \cdot \hat{n} + \gamma\beta]\hat{\beta}}{\gamma(1 + \beta \cdot \hat{n})},$$

$$\gamma = (1 - \beta^2)^{-1/2}, \quad (1)$$

where the primed coordinate system refers to the aberrated (Earth) viewpoint. A uniform blackbody temperature field, T , aberrates (Peebles & Wilkinson 1968) into a blackbody temperature field $T'(\hat{n}')$ according to

$$T'(\hat{n}') = \frac{T}{\gamma(1 - \beta \cdot \hat{n}')}.$$
(2)

To aberrate a general temperature field $T(\hat{n})$, we substitute T with $T(\hat{n})$, since light viewed along \hat{n}' in the aberrated view is viewed along \hat{n} in the unaberrated view, where \hat{n} and \hat{n}' are related by equation (1),

$$T'(\hat{n}') = \frac{T(\hat{n})}{\gamma(1 - \beta \cdot \hat{n}')}.$$
(3)

Consequently, by aberrating with velocity $-\beta$ the equation for the deaberrated temperature field is obtained:

$$T(\hat{n}) = \frac{T'(\hat{n}')}{\gamma(1 + \beta \cdot \hat{n})},$$
(4)

where \hat{n}' is a function of \hat{n} given by equation (1). Note that as a consistency check, equation (3) can be substituted in the right-hand side of equation (4) to give $T(\hat{n})/[\gamma^2(1 - \beta \cdot \hat{n}')(1 + \beta \cdot \hat{n})]$, which simplifies to $T(\hat{n})$ using equation (1).

Given a pixelized map, equation (4) can be used to construct a deaberrated map provided a way is found to interpolate between pixels. It is reasonable to do this because the spread of the beam profile of the observing instrument ensures that the map is nearly band-limited. The interpolation could be achieved using a spherical harmonic analysis of the map, $T'(\hat{n}') = \sum a'_{lm} Y_{lm}(\hat{n}')$, calculated for instance using HEALPIX (Górski et al. 1999).

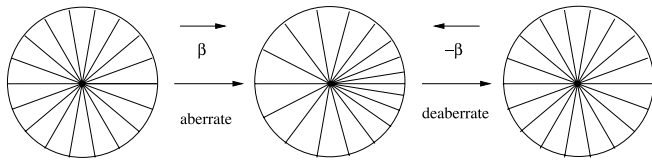


FIG. 1.—Deaberration restores light rays to unaberrated directions.

Such interpolation does not account for the incomplete sky coverage, however. Localized interpolation could be achieved, for example, by using bicubic interpolation, but some uncertainty would remain.

It would be better to construct the deaberrated map directly from the raw time-ordered data produced by the observing instrument. Pixelization occurs at the end of this process and so the need to interpolate is eliminated. Typically, CMB instruments produce output from several spectral channels, from which temperature is calculated; see, e.g., the *WMAP* experiment (Hinshaw

TABLE 1
CORRECTED GALACTIC COORDINATES AND REDSHIFT FOR THE 50 MOST ABERRATED OBJECTS WITH $z > 1$ ($\cos \Delta\theta = \hat{n} \cdot \hat{n}'$)

Name	l (deg)	b (deg)	z	$\Delta\theta$	Δz
ERO J164023+4644.0	72.67080	41.39394	1.049001	0.07047	0.000001
PKS 0230–790.....	297.14998	–37.26604	1.069995	0.07047	–0.000005
[MYF99] J0917+8142c.....	130.71970	31.78057	1.070000	0.07047	0.000000
PC 1639+4628	72.19289	41.26659	1.304997	0.07047	–0.000003
[HB89] 1831–711.....	323.73096	–24.51449	1.356005	0.07047	0.000005
[MYF99] J0923+8149a.....	130.46658	31.89165	1.389999	0.07047	–0.000001
RX J1541.2+7126.....	106.64072	39.82372	1.418003	0.07047	0.000003
[HB89] 1700+180.....	38.16213	31.73087	1.423991	0.07047	–0.000009
2MASSi J0453023–333359.....	235.69337	–38.26683	1.800004	0.07047	0.000004
[MYF99] J0917+8142a.....	130.72920	31.79118	1.859999	0.07047	–0.000001
[MYF99] J0917+8142b.....	130.72479	31.78714	1.869999	0.07047	–0.000001
HE 0442–4445.....	249.88261	–40.97861	1.918008	0.07047	0.000008
PMN J0459–2330.....	223.98060	–34.50293	1.989999	0.07047	–0.000001
Abell 2219: [FBB2002] 1.....	72.69397	41.42281	4.068000	0.07047	0.000000
Abell 2219: [FBB2002] 2.....	72.67086	41.41442	4.444999	0.07047	–0.000001
Abell 2219: [FBB2002] 3.....	72.62727	41.42965	4.654002	0.07047	0.000002
[HB89] 1642+409.....	64.92009	40.66151	1.300017	0.07047	0.000017
[HB89] 0448–392.....	242.74590	–39.67631	1.302014	0.07047	0.000014
87GB 160847.5+654032.....	98.32452	40.82205	1.393985	0.07047	–0.000015
[HB89] 1642+411.....	65.15790	40.69027	1.436017	0.07047	0.000017
PMN J0438–4728.....	253.64664	–41.76199	1.444988	0.07047	–0.000012
[HB89] 1643+406.....	64.45374	40.58646	1.451012	0.07047	0.000018
HS 0621+6738.....	147.11385	22.61153	1.588012	0.07047	0.000012
[HB89] 1642+412.....	65.22351	40.64394	1.970004	0.07047	0.000010
[HB89] 0447–395.....	243.11944	–39.80981	1.980002	0.07047	0.000008
CTS 0514.....	254.19202	–41.27335	2.369995	0.07047	0.000016
2MASSi J0446589–414601.....	246.06335	–40.36583	2.700013	0.07047	0.000013
[HB89] 1640+471.....	73.13984	41.19657	2.763979	0.07047	–0.000021
2MASSi J0445327–404848.....	244.79364	–40.58809	3.269976	0.07047	–0.000024
PC 1640+4628.....	72.17494	41.11833	3.694976	0.07047	–0.000024
PC 1636+4635.....	72.37277	41.74207	1.2220051	0.07047	0.000012
[HB89] 1642+410 NED02.....	64.98530	40.79491	1.240010	0.07047	0.000016
[HB89] 1642+401.....	63.76762	40.56944	1.268022	0.07047	0.000022
[HB89] 1642+410 NED03.....	65.03083	40.77975	1.370022	0.07047	0.000022
[HB89] 1643+400.....	63.74611	40.48168	1.877022	0.07047	0.000022
CTS 0648.....	258.06942	–41.39991	2.940036	0.07047	0.000036
PKS 0454–234.....	223.67308	–34.96014	1.002978	0.07047	–0.000022
3C 305.1.....	114.89062	38.26538	1.132022	0.07047	0.000022
CXOU J031015.9–765131.....	293.55532	–37.68363	1.187022	0.07047	0.000022
HE 0435–5304.....	261.02111	–41.44491	1.231026	0.07047	0.000026
[HB89] 1642+400.....	63.68701	40.64412	1.377027	0.07047	0.000027
CADIS 16h–0604.....	85.22938	42.44569	1.430025	0.07047	0.000025
[HB89] 1641+411.....	65.10552	40.85849	1.570027	0.07047	0.000027
[HB89] 1643+395.....	63.01211	40.46099	2.145031	0.07047	0.000031
[HB89] 1641+410.....	64.98338	40.86438	2.385037	0.07047	0.000037
MS 1006.3+8212.....	129.02387	33.12097	2.410037	0.07047	0.000033
CADIS 16h–0330.....	85.08463	42.44283	2.410033	0.07047	0.000033
HS 1649+3905.....	62.59049	39.32292	3.165949	0.07047	–0.000051
CADIS 16h–0780.....	85.05864	42.47427	3.720048	0.07047	0.000048
CADIS 16h–2028.....	85.17524	42.54781	1.130027	0.07047	0.000027

et al. 2003). The direction \hat{n}' of a raw observation should be modified to its deaberrated direction \hat{n} . This is achieved by aberrating \hat{n}' with velocity $-\beta$ so that equation (1) transforms to

$$\hat{n} = \frac{\hat{n}' + [(\gamma - 1)\hat{\beta} \cdot \hat{n}' - \gamma\hat{\beta}]\hat{\beta}}{\gamma(1 - \hat{\beta} \cdot \hat{n}')}.$$
 (5)

The deaberrated temperature, using equation (3), is

$$T(\hat{n}) = \gamma(1 - \hat{\beta} \cdot \hat{n}')T'(\hat{n}').$$
 (6)

The deaberrated data can then be used to construct a pixelized map in the same way a map would be constructed without deaberration.

3. DEABERRATING ASTROPHYSICAL OBJECTS

In the case of objects, we first wish to know the deaberrated line-of-sight object direction \hat{n} from the observed aberrated object direction \hat{n}' . This has already been given in equation (5). The Doppler effect when aberrating the line-of-sight \hat{n} is (Calvao 2004)

$$\nu' = \nu\gamma(1 + \hat{\beta} \cdot \hat{n}).$$
 (7)

The deaberrated frequency, in terms of the observed \hat{n}' , is then

$$\nu = \nu'\gamma(1 - \hat{\beta} \cdot \hat{n}'),$$
 (8)

and the desired deaberrated spectral redshift is

$$z = \frac{\nu_0}{\nu - 1} = \frac{\nu_0/\nu'}{\gamma(1 - \hat{\beta} \cdot \hat{n}')} = \frac{z' + 1}{\gamma(1 - \hat{\beta} \cdot \hat{n}') - 1},$$
 (9)

where ν_0 is the unredshifted spectral line frequency. The aberration of the photon number density spectrum from Peebles & Wilkinson (1968) is

$$n'(\nu', \hat{n}') = n(\nu, \hat{n})(\nu'/\nu)^2,$$
 (10)

so the intensity spectrum $I(\nu, \hat{n}) = \hbar\nu n(\nu, \hat{n})$ aberrates to

$$I'(\nu', \hat{n}') = I(\nu, \hat{n})(\nu'/\nu)^3.$$
 (11)

Hence, the deaberrated spectra are

$$n(\nu, \hat{n}) = n'(\nu', \hat{n}')/[\gamma(1 + \hat{\beta} \cdot \hat{n})]^2,$$
 (12)

$$I(\nu, \hat{n}) = I'(\nu', \hat{n}')/[\gamma(1 + \hat{\beta} \cdot \hat{n})]^3,$$
 (13)

where ν' is given by equation (7) and \hat{n}' by equation (1).

Using these formulae, we have prepared a table of deaberrated objects from an initial table of all objects with $z > 1.0$ taken from NASA/IPAC Extragalactic Database.¹ Our deaberrated table can be found at the authors' Web site.² For illustration, Table 1 summarizes the 50 objects with the largest angular aberration correction (but low redshift correction).

4. FURTHER PECULIARITIES

For greater accuracy, we must account for the variation in peculiar velocity caused by the earth's rotation and movement about the Sun, which is $\approx 5\%$ of the total. To do this either the original observation must have been corrected for this variation, or we must know the time when the observation was taken and add to the average value of β the velocity of the earth relative to the Sun at this time.

5. SUMMARY

Formulae have been given for constructing deaberrated CMB maps and object surveys. These could be applied one time prior to an application of tests that require a view point that is at rest relative to the comoving Hubble flow. Otherwise, each process must be modified and will suffer an increase in complexity and computational cost. Processes currently of interest are searches for nontrivial compact topology, and in the future tests of non-Gaussianity and analysis of weak lensing. Other tests will also undoubtedly arise as the precision of cosmological data increases.

The authors wish to thank the referee for finding errors and suggesting improvements. Work at the University of Notre Dame supported by the US Department of Energy under research grant DE-FG02-95-ER40934, and a University of Notre Dame Center for Applied Mathematics (CAM) summer fellowship. This research has made use of the NASA/IPAC Extragalactic Database (NED), which is operated by the Jet Propulsion Laboratory, California Institute of Technology, under contract to the National Aeronautics and Space Administration.

¹ Available at: <http://nedwww.ipac.caltech.edu>.

² Available at: www.nd.edu/~dmenzies/deab.

REFERENCES

- Calvao, M. O. 2004, preprint (astro-ph 0404536)
 Challinor, A., & van Leeuwen, F. 2002, Phys. Rev. D, 65, 103001
 Cornish, N. J., Spergel, D. N., & Starkman, G. 1998, Phys. Rev. D, 57, 5982
 Górski, K. M., Hivon, E., & Wandelt, B. D. 1999, in Proc. MPA/ESO Conference on Evolution of Large-Scale Structure: from Recombination to Garching, ed. A. J. Banday, R. K. Sheth, & L. Da Costaastro (Garching: ESO), 37
 Hinshaw, G., et al. 2003, ApJS, 148, 63
 Levin, J. 2004, preprint (astro-ph 0403036)
 Lineweaver, C. H. 1997, in Microwave Background Anisotropies: Proc. XVIth Moriond Astrophysics Meeting, ed. F. R. Bouchet et al. (Gif-sur-Yvette: Editions Frontières), 69
 Peebles, P. J. E., & Wilkinson, D. T. 1968, Phys. Rev., 174, 2168